Mol Cell Biochem
DOI 10.1007/s11010-017-3186-7

APE1 modulates cellular responses to organophosphate pesticide-induced oxidative damage in non-small cell lung carcinoma A549 cells

Shweta Thakur[1] · Monisha Dhiman[2] · Anil K. Mantha[1]

Received: 6 June 2017 / Accepted: 1 September 2017

Abstract Monocrotophos (MCP) and chlorpyrifos (CP) are widely used organophosphate pesticides (OPPs), speculated to be linked with human pathologies including cancer. Owing to the fact that lung cells are most vulnerable to the environmental toxins, the development and progression of lung cancer can be caused by the exposure of OPPs. The present study investigates the oxidative DNA damage response evoked by MCP and CP in human non-small cell lung carcinoma A549 cells. A549 cells were exposed to MCP and CP; cytotoxicity and reactive oxygen species (ROS) generation were measured to select the non-toxic dose. In order to establish whether MCP and CP can initiate the DNA repair and cell survival signalling pathways in A549 cells, qRT-PCR and Western blotting techniques were used to investigate the mRNA and protein expression levels of DNA base excision repair (BER)-pathway enzymes and transcription factors (TFs) involved in cell survival mechanisms. A significant increase in cell viability and ROS generation was observed when exposed to low and moderate doses of MCP and CP at different time points (24, 48 and 72 h) studied. A549 cells displayed a dose-dependent accumulation of apurinic/apyrimidinic (AP) sites after 24 h exposure to MCP advocating for the activation of AP endonuclease-mediated DNA BER-pathway. Cellular responses to MCP- and CP-induced oxidative stress resulted in an imbalance in the mRNA and protein expression of BER-pathway enzymes, viz. PARP1, OGG1, APE1, XRCC1, DNA pol β and DNA ligase III α at different time points. The treatment of OPPs resulted in the upregulation of TFs, viz. Nrf2, c-jun, phospho-c-jun and inducible nitric oxide synthase. Immunofluorescent confocal imaging of A549 cells indicated that MCP and CP induces the translocation of APE1 within the cytoplasm at an early 6 h time point, whereas it promotes nuclear localization after 24 h of treatment, which suggests that APE1 subcellular distribution is dynamically regulated in response to OPP-induced oxidative stress. Furthermore, nuclear colocalization of APE1 and the TF c-jun was observed in response to the treatment of CP and MCP for different time points in A549 cells. Therefore, in this study we demonstrate that MCP- and CP-induced oxidative stress alters APE1-dependent BER-pathway and also mediates cell survival signalling mechanisms via APE1 regulation, thereby promoting lung cancer cell survival and proliferation.

Keywords Monocrotophos · Chlorpyrifos · APE1 · BER-pathway · ROS

Introduction

Organophosphate pesticides (OPPs) are widely employed in agricultural, industrial and household purposes. Their substantial exposure leads to toxicity by acting as acetylcholinesterase (AChE) inhibitors and disrupting neuromuscular transmission; also they have been reported to cause oxidative stress and DNA damage in experimental animals and tissue culture studies [1, 2]. OPP poisoning has been reported to manifest into human pathologies such as

✉ Anil K. Mantha
anilmantha@gmail.com; anil.kumar@cup.ac.in

[1] Centre for Animal Sciences, School of Basic and Applied Sciences, Central University of Punjab, Bathinda, Punjab 151 001, India

[2] Centre for Biochemistry and Microbial Sciences, School of Basic and Applied Sciences, Central University of Punjab, Bathinda, Punjab, India

Published online: 08 September 2017

asthma, neurological dysfunction, birth defects and others [3, 4]. Repeated low or heavy exposure of OPPs-induced reactive oxygen species (ROS) generation can lead to tumour promotion and carcinogenesis. Research indicates that OPPs increase cancer risk [5, 6]. Among all cancers, risk of lung cancer development and progression due to acute or chronic toxicity of OPPs is more for the reason that lung cells are easily exposed and vulnerable through inhalation of vapours, airborne droplets or concentrated wettable powder form. Also, advanced-stage diagnosis and limited treatment interventions advocate for a much needed research for lung cancer. Among OPPs, monocrotophos (MCP) and chlorpyrifos (CP) are the most commonly used pesticides. Genotoxicity of MCP has been explored in mice [7] and shown to induce MCF7 breast cancer cell proliferation [8]. MCP induces the production of ROS and induces apoptosis in neuronal PC12 cells [9]. Another investigation suggests that CP increases the number of micronuclei in mouse hepatocytes [10]. Dose-dependent CP-induced DNA damage was also observed in mice leucocytes [11]. Very recently, it was demonstrated that CP causes significant ROS generation, chromosomal aberrations, apoptosis, micronucleus induction and also alterations in cell cycle in bone marrow cells derived from the swiss albino mice [12].

After genotoxic assault, the ability to recognize DNA damage, initiate and coordinate the DNA repair pathways until completion is important. Base excision repair (BER)-pathway is the predominant one against oxidative base damages in the genome, viz. oxidized bases, apurinic/apyrimidinic (AP) sites, single-strand breaks (SSBs) generated exogenously due to environmental toxins including OPPs. BER-pathway involves monofunctional DNA glycosylase (DG) that removes the damaged base generating AP site, which is then recognized and incised by the key regulator enzyme AP endonuclease 1 (APE1), or bifunctional DNA glycosylase/8-oxoG-DNA glycosylase (OGG1) with additional AP lyase activity that cleaves the AP site and leaves the unsaturated abasic terminus, to be finally processed by APE1. APE1 also recruits other downstream BER-pathway proteins such as X-ray repair cross-complementing group 1 (XRCC1) which act as a scaffold for protein–protein interactions, DNA polymerase β (DNA pol β) and DNA ligase III α; thus, it helps in coordinating the short-patch/single-nucleotide BER (SN-BER) process. Poly (ADP-ribose) polymerase 1 (PARP1) is another important BER-pathway enzyme which acts as a DNA damage sensor as well as a signalling molecule and plays a role in long-patch BER (LP-BER) process [13–15]. Defects in BER-pathway have also been linked with various types of cancer such as decreased activity of OGG1 which has been linked with lung cancer risk [16]. APE1 exerts its repair function through its endonuclease activity on the AP sites of DNA via C-terminal domain, whereas the N terminus contains the nuclear localization signal (NLS), and it also mediates transcriptional redox regulation of various transcription factors (TFs) such as activator protein 1 (AP-1), nuclear factor-kappaB (NF-κB) and nuclear factor erythroid 2-related factor 2 (Nrf2) associated with cell survival mechanisms as reviewed elsewhere extensively [17–19]. Considering that APE1 repairs the damaged DNA as well as reductively activates key TFs controlling gene expression necessary for cell survival, it may not be confounding that the altered expression levels and activities of APE1 have been linked with various cancers [20, 21]. Studies have reported the association links between the altered expression of APE1 and lung cancer [22, 23]. Variation in the subcellular distribution of APE1 in response to oxidative stress is another important perspective. APE1′s prime localization in the nucleus accounts for its cellular response to oxidative stress and regulation of cell proliferation rate, whereas increased cytoplasmic expression has also been associated with various tumorigenic processes [24], particularly lung cancer [25]. Although studies have shown that MCP and CP cause oxidative stress and have genotoxic potential, still the evidence regarding MCP- and CP-mediated dysregulation in DNA repair and cell survival signalling pathways, and their correlation in enhancing the risk for lung cancer progression, is inadequate. The results of the present study indicate the possible mechanisms by which the MCP and CP induce oxidative stress and the DNA damage intervenes the APE1-mediated BER-pathway and regulation of pro-survival signalling pathways, thus helping lung cancer cells to survive and proliferate.

Materials and methods

Cell culture and treatments

Human alveolar basal epithelial carcinoma A549 cells were originally procured from the National Centre for Cell Sciences (NCCS), Pune, India and have been maintained at the tissue culture laboratory, Central University of Punjab, Bathinda (CUPB), India, as per the standard protocols. A549 cells were grown in Dulbecco's Modified Eagle's Medium (DMEM) supplemented with 10% foetal bovine serum (FBS) and 1 × penicillin and streptomycin (P/S) in a humidified incubator with 5% CO_2 at 37 °C. Using trypan blue dye exclusion assay, A549 cells were checked for their viability prior to all experiments.

The main stocks of 50 mM of both MCP and CP (Sigma-Aldrich, PESTANAL, analytical grade) were prepared in water (H_2O) and 100% dimethylsulphoxide (DMSO), respectively. Control samples consisted of

untreated cells for MCP and cells treated with 0.1% DMSO for CP as a vehicle control [9, 26].

Selection of non-cytotoxic doses

Prior to using A549 cells further for expression studies, non-toxic doses of MCP and CP were identified using [3-(4, 5-dimethylthiazol-2-yl)-2, 5-diphenyltetrazolium bromide] (MTT) assay. Briefly, A549 cells (1×10^4 cells/well) were seeded in 96-well plates and incubated in the CO_2 incubator for 18–24 h at 37 °C. Then the medium was aspirated and serum starvation was carried out for 12 h. After that, the cells were exposed to serum-free DMEM medium containing MCP and CP (0.01–500 μM) for 24, 48 and 72 h. Selection of MCP and CP concentrations was based on previous studies with A549 and other cell lines [9, 26].

Determination of reactive oxygen species (ROS)

Total ROS levels were assessed following the exposure of MCP and CP (0.01, 1, 10 and 100 μM) to A549 cells for 6 and 24 h using CellROX Deep Red reagent. A549 cells were seeded in 48-well plates at 0.025×10^6 density, treated with MCP and CP for 6 and 24 h time points and then incubated with 10 μM CellROX^{TM} Deep Red (Invitrogen) at 37 °C for 1 h. The microplate reader was used to detect CellROX Deep Red-loaded cells at an excitation wavelength of 644 nm and an emission wavelength of 665 nm [27].

Simultaneously, fluorescence imaging employing 2′, 7′ dichlorodihydrofluorescein diacetate (H_2DCF-DA) dye was used to confirm intracellular ROS generation. Cells were grown on coverslips, allowed to adhere and exposed to MCP and CP (0.01, 0.1, 1, 10 and 100 μM) for 6 h. After the treatment, A549 cells were washed with 1x PBS and incubated with serum-free DMEM media containing 20 μM H_2DCF-DA (Invitrogen). Coverslips were then washed twice with 1× PBS, mounted and analysed using an FSX100 fluorescent microscope (Olympus) [28].

Estimation of apurinic/apyrimidinic (AP) sites

AP sites, a prevalent type of oxidative DNA base lesions, were determined in total DNA isolated from MCP-treated (0.1, 1, 10 and 100 μM for 24 h) A549 cells using OxiSelect^{TM} oxidative DNA damage AP sites quantitation kit (Cell Biolabs, USA) as per the manufacturer's protocol. The kit is based on the aldehyde reactive probe (ARP) that specifically binds with aldehyde group on the open ring form of AP sites, followed by biotin detection coupled to streptavidin. Detection was performed by measuring O.D. at 450 nm and the number of AP sites per 100,000 base pairs in each sample was calculated using ARP standard curve [29].

Total RNA extraction and real-time PCR (qRT-PCR) analysis

Total RNA extraction was performed using MCP- and CP-treated (10 μM) A549 cells at indicated time points using TRIzol reagent (Invitrogen) as per manufacturer's protocol. Quantification of isolated RNA was performed by UV spectrophotometry. For each sample, 1 μg of RNA was reverse-transcribed into cDNA by SuperScript III first-strand cDNA synthesis kit (Invitrogen). Quantitative real-time PCR (qRT-PCR) was conducted on an Applied Biosystems StepOnePlus Real-Time PCR system using the VeriQuest SYBR Green qPCR master mix (Affymetrix). The reactions were carried out in triplicates for each sample with standard reaction volume of 12 μL. The steps included a 2-min hold at 50 °C for UDG treatment, a 10-min hold at 95 °C for Taq DNA polymerase activation and UDG inactivation, then PCR amplification cycles ($n = 35$) of denaturation (95 °C, 15 s), annealing and extension (55–60 °C, 30–60 s). The primer specificity was assessed by melting curve analysis and NTCs for respective primers. Data were normalized using β-actin as an endogenous control. Relative change in mRNA expression was analysed using comparative $2^{-\Delta\Delta CT}$ method and is expressed as fold change keeping the values of unexposed controls as basal (i.e. 1) [30]. The primer sequences for BER-pathway enzymes determined that were designed using Primer3 tool and procured from Imperial Life Sciences (ILS) are listed in Table 1.

Preparation of total cell lysates and Western blot analysis

A549 cells were seeded at a density of 2.5×10^6 cells onto 100 mm dishes and treated with MCP and CP (0.1, 1, 10 and 100 μM). Following exposure, the cells were pelleted and lysed with 400–500 μL of modified RIPA lysis buffer [50 mM Tris–HCl (pH 7.4), 150 mM NaCl, 1 mM EDTA, 1% NP-40, protease inhibitor cocktail (Sigma; 1 μL per 100 μL of lysis buffer)] [31]. The protein concentration was determined using Bradford assay. Sixty micrograms of protein per well was resolved on 10% SDS polyacrylamide gel electrophoresis (SDS-PAGE) and transferred onto a PVDF membrane. Ponceau S staining was performed to confirm equal loading of the protein samples. Membranes were blocked at room temperature for 1–2 h with TBS containing 5% non-fat dry milk (NFDM) and 0.1% Tween 20 (NFDM-TBST). Membranes were then incubated for overnight at 4 °C with primary antibodies: APE1/Ref-1, PARP-1, XRCC1, DNA pol β, c-jun, p-c-jun (Ser 63),

Table 1 List of primer sequences used for qRT-PCR

Gene Name	Forward sequence (5′–3′)	Reverse sequence(5′–3′)
APE1	TGGAATGTGGATGGGCTTCGAGCC	AAGGAGCTGACCAGTATTGATGA
PARP1	CCCAGGGTCTTCGGATAG	AGCGTGCTTCAGTTCATACA
XRCC1	GGGACCGGGTCAAAATTGTT	ACCGTACAAAACTCAAGCCAAAG
OGG1	ACTTATCATGGCTTCCCAAACC	CAACTTCCTCAGGTGGGTCTCT
DNA Pol β	GGCAGTTTCAGAGGTGC	GGCAAACACCCATGAACTTT
DNA ligase III α	GATCACGTGCCACCTACCTTGT	GGCATAGTCCACACAGAACCGT
β-actin	CTAAGTCATAGTCCGCCTAGAAGCA	TGGCACCCAGCACAATGAA

NOS2, Nrf2, β-actin, GAPDH (Santa Cruz, 1:1000 dilution) and OGG1 (Novus Biologicals, 1:1000 dilution) in 5% NFDM-TBST. After three washings in TBST for 5 min each, membranes were then incubated for 1 h at room temperature with respective HRP-conjugated anti-mouse IgG and anti-rabbit IgG secondary antibody (Invitrogen and Genei) at a dilution of 1:5000–1:10,000 in 5% NFDM-TBST. Detection was performed using Bio-Rad Clarity™ ECL reagent. Images were captured by ChemiDoc MP or FluorChem HD2 (Protein Simple) systems and densitometry was carried out using Image Lab or ImageJ Software.

Immunofluorescence and colocalization study of APE1 with the transcription factor c-jun

Subcellular distribution of APE1 as well as its colocalization with c-jun was examined using immunofluorescence analysis by confocal laser scanning microscopy (CLSM). For this, A549 cells were seeded onto glass coverslips and treated with MCP and CP (0.01 and 10 μM) for 6, 12, 24, 48 and 72 h time points. Cells were then fixed with 2% paraformaldehyde (PFA) in PBS for 10 min at room temperature, permeabilized with 0.1% Triton X-100 in PBS for 5 min and then blocked with 1× PBS containing 10% FBS for 30 min. The cells on coverslips were then incubated with primary anti-APE1/Ref-1 mouse monoclonal antibody and anti-c-jun rabbit polyclonal (dilution 1:100) in 1× PBS containing 0.1% Triton X-100 and 10% FBS, overnight at 4 °C, washed with 1× PBS three times for 5 min and incubated with FITC-labelled Alexa Fluor 488 anti-mouse and Alexa Fluor 647 anti-rabbit secondary antibody (Invitrogen) at 1:100 dilution in 1× PBS containing 0.1% Triton X-100 and 10% FBS, at 37 °C for 90 min. The coverslips were then washed three times with 1× PBS and cell nuclei were stained with DAPI for 30 min at 37 °C. Coverslips were then washed once with 1× PBS and mounted on microscopic glass slides [32]. The fluorescence image of the stained nuclei and the immunofluorescence images of APE1/Ref-1 and c-jun were captured using CLSM (Olympus FV1200) at the Central Instrumentation Laboratory (CIL) facility of CUPB. Fluorescence colocalization analysis of APE1 and c-jun was performed using Pearson's correlation coefficient (PCC) that ranges from +1 (perfect positive correlation) to −1 (perfect negative correlation) [33].

Statistical analysis

Data were presented as mean value ± standard deviation (SD) and mean ± standard error mean (SEM). Statistical analysis was performed using paired Student's two-tailed *t* test to compare the results of control and experimental samples. $*P$ value <0.05, $**P$ value <0.01 and $***P$ value <0.001 were considered statistically significant.

Results

Assessment of cell viability by MTT assay

To estimate the effect of CP- and MCP-induced oxidative stress, and prior to using further for expression studies, toxic and non-toxic doses were identified using MTT assay. A549 cells were exposed to 0.01, 0.1, 1, 10, 100 and 500 μM CP and MCP concentrations and tested for cytotoxicity after 24, 48 and 72 h. Treatment of CP did not cause notable cytotoxicity in A549 cells between the doses of 0.01 and 100 μM after 24 and 48 h time points, but 500 μM CP caused a significant reduction in cell viability by 57 and 50% ($P < 0.01$) at 24 and 48 h time points, respectively (Fig. 1a). However, exposure to CP at 1, 10 and 100 μM for 48 h time point resulted in a significant increase in cell viability (22, 27 and 20%, respectively) ($P < 0.05$). Further treatment with MCP resulted in a significant increase by 13 and 21% in proliferation at 10 and 100 μM concentrations, respectively, for 24 h ($P < 0.001$), whereas a slight decrease in proliferation was observed at 1, 10 and 100 μM MCP ($P < 0.05$) for 48 h, as compared to untreated control A549 cells (Fig. 1b). However, exposure to a high MCP concentration (500 μM) was found to be cytotoxic (96% reduction in cell viability) at the 72 h time point. Amidst all concentrations at 72 h exposure, 10 μM MCP resulted only in a 5% decrease in cell

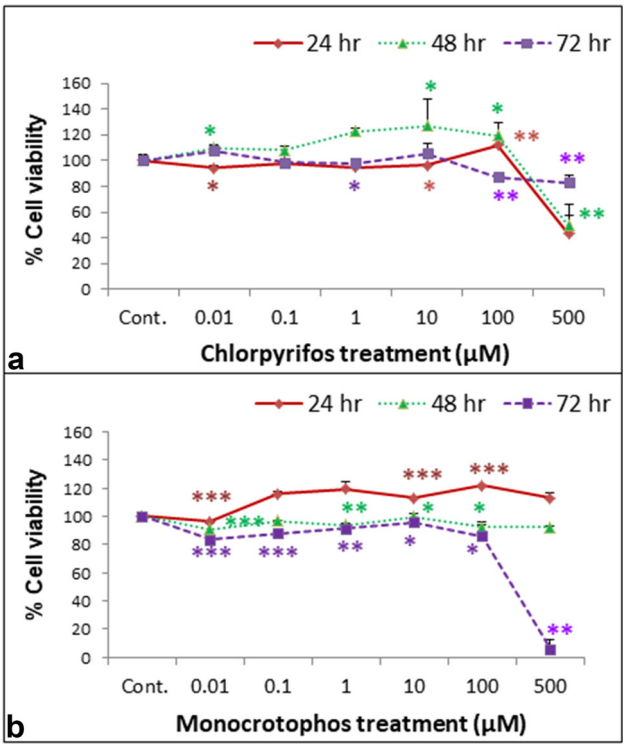

Fig. 1 Cytotoxicity of **a** chlorpyrifos (CP) and **b** monocrotophos (MCP) in A549 cells. A549 cells were exposed to CP and MCP (0.01, 0.1, 1, 10, 100 and 500 μM) for 24, 48 and 72 h before measuring cytotoxicity using MTT assay. Results were expressed as mean % cell viability relative to untreated/DMSO control ± standard deviation ($n = 3$; *P value <0.05, **P value <0.01 and ***P value <0.001)

viability, whereas 0.01, 0.1, 1 and 100 μM resulted in 17, 12, 9 and 14% reduction in cell viability, respectively. Therefore, it can be stated that exposure to lower concentrations of CP and MCP favours cell survival at 24 and 48 h time points studied, probably due to activation of pro-survival pathways.

Estimation of intracellular ROS using CellROX deep red and H_2DCF-DA

Exposure to oxidants and environmental toxins result in oxidative stress. Therefore, we intended to estimate ROS generation using CellROX Deep Red and H_2DCF-DA assays. Statistically significant ($P < 0.05$) ROS generation was observed in A549 cells treated with CP and MCP (0.01, 0.1, 1 and 10 μM) for 24 h (Fig. 2a, b). Exposure to CP (10 μM) induced a maximum of 82% increase in ROS followed by 81% (1 μM) and 66% (0.01 μM), whereas MCP (10 μM) exposure induced a maximum of 95% increase in ROS followed by 94% (1 μM) and nearly 79% (0.01 μM) change in ROS levels as compared with that of the untreated control A549 cells. A significant increase in ROS generation was also observed for 6 h exposure to both CP and MCP at 0.01, 0.1, 1 and 10 μM concentrations studied, but the response in elevation of ROS was found to be less as compared to 24 h of exposure to A549 cells.

In addition, the change in intracellular ROS generation in A549 cells was also recorded microscopically using fluorescent H_2DCF-DA dye at 6 h early time point. As compared to the untreated A549 cells, the fluorescence intensity was observed to be increased with an increase in the concentration of CP (0.1–100 μM). Further, treatment of the A549 cells with MCP (0.1–100 μM) displayed a stronger response in the generation of intracellular ROS than that of CP treatment for the same concentrations at the 6 h time point (Fig. 2c).

Estimation of apurinic/apyrimidinic (AP) sites

To evaluate the extent of oxidative DNA damage upon treatment with MCP in A549 cells, we measured the number of AP sites, one prevalent type of oxidative DNA base lesion, using aldehyde reactive probe (ARP) assay using the genomic DNA extracted from the A549 cells. As shown in Fig. 3, a significant dose-dependent ($P < 0.05$) increase in accumulation of number of AP sites (18, 21, 22 and 36%) was observed in genomic DNA of A549 cells treated with 0.1, 1, 10 and 100 μM concentrations of MCP, respectively, for 24 h time point, which might be a resultant effect of MCP-induced oxidative stress in A549 cells.

Determination of transcriptional and translational levels of BER-pathway enzymes

Oxidative stress alters the functionality of BER-pathway. qRT-PCR and Western blotting techniques were carried out to understand the mRNA and protein expression patterns of individual enzymes of the BER-pathway in response to OPP-induced oxidative stress at different time points.

qRT-PCR analysis

CP- and MCP-induced changes in the mRNA expression levels of BER-pathway genes in A549 cells are presented in Fig. 4. For 10 μM CP exposure, significant upregulation in the mRNA level of *APE1* by 1.4 fold ($P < 0.001$) and *PARP1* by 2 fold after 24 h of treatment was observed, whereas upregulation in the *mRNA* level of *DNA ligase III* α by 1.7-fold was found after 48 h of treatment. For MCP treatment, an increase in the *mRNA* level of *APE1* by 1.3- and 1.13-fold ($P < 0.05$) was observed after 12 and 48 h of treatment, respectively. *PARP1* expression level was found to be upregulated (1.14- and 1.5-fold) after 24 and 48 h of treatment, respectively. Significant upregulation in the

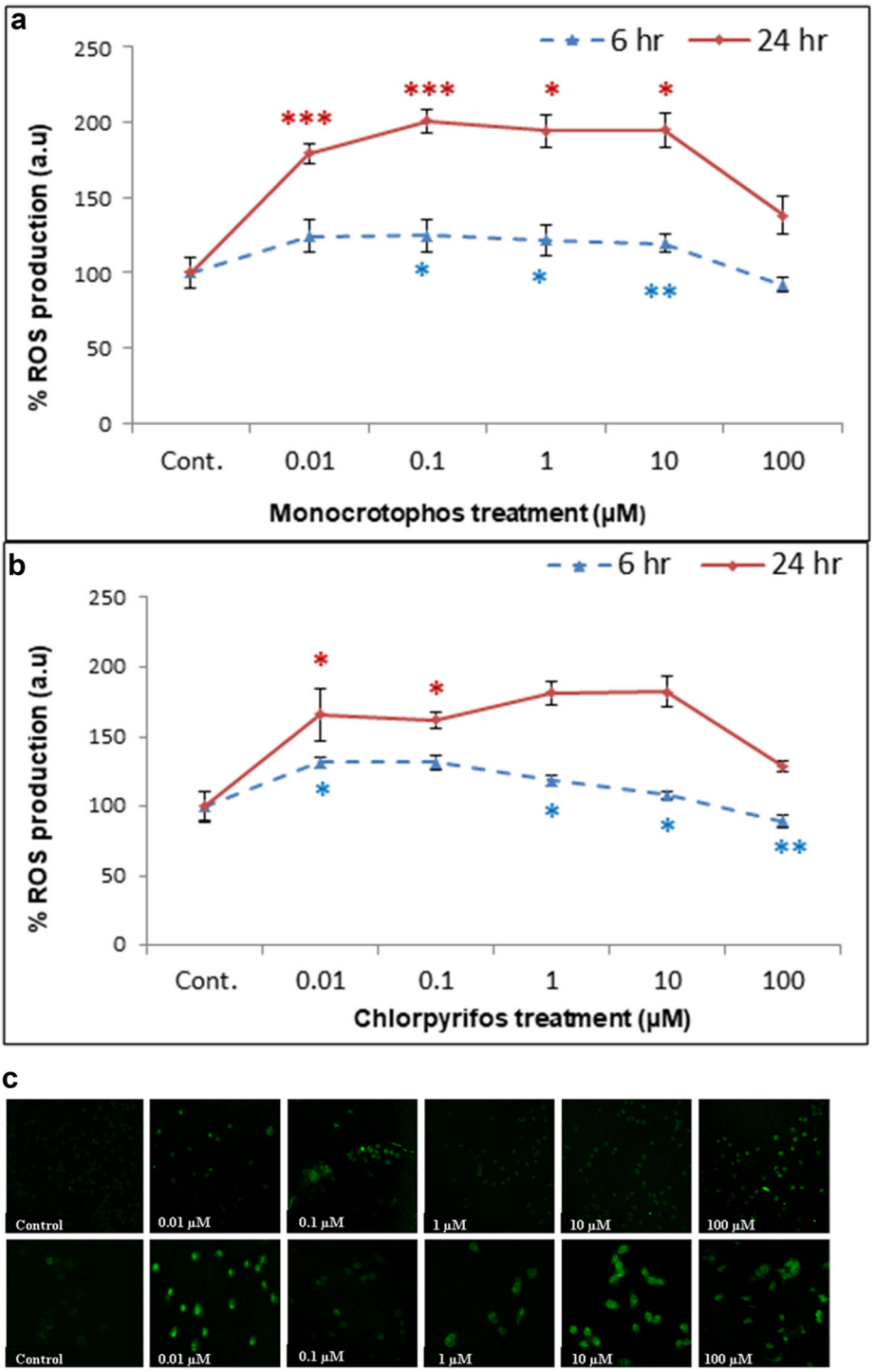

Fig. 2 ROS production in **a** monocrotophos (MCP)- and **b** chlorpyrifos (CP)-treated A549 cells. A549 cells were exposed to MCP and CP (0.01, 0.1, 1, 10 and 100 μM) for 6 and 24 h before measuring the ROS production using CellROX Deep Red assay. Results were expressed as % change in ROS production relative to untreated/DMSO control ± standard deviation ($n = 3$; *P value < 0.05, **P value < 0.01 and ***P value < 0.001). **c** Representative microphotographs showing CP- and MCP-induced ROS in A549 cells after 6 h of exposure. ROS generation was studied using H_2DCF-DA dye and the images were acquired using a FSX100 fluorescent microscope (Olympus)

mRNA level of *DNA ligase III* α (2.4-fold) was observed after 48 h of exposure to MCP. The expression pattern of *OGG1* was almost the same in both CP and MCP (10 μM) treatment of A549 cells. Contrary to other BER enzymes, the DG *OGG1* expression level was found to be significantly downregulated by 90, 80 and 87% after 6, 24 and 48 h of CP treatment and by 91, 67 and 28% at 6, 24 and 48 h of MCP treatment, respectively. The results obtained in the present study suggest that the *mRNA* expression levels of BER-pathway enzymes are dynamically regulated in response to the OPP-induced oxidative stress in A549 cells.

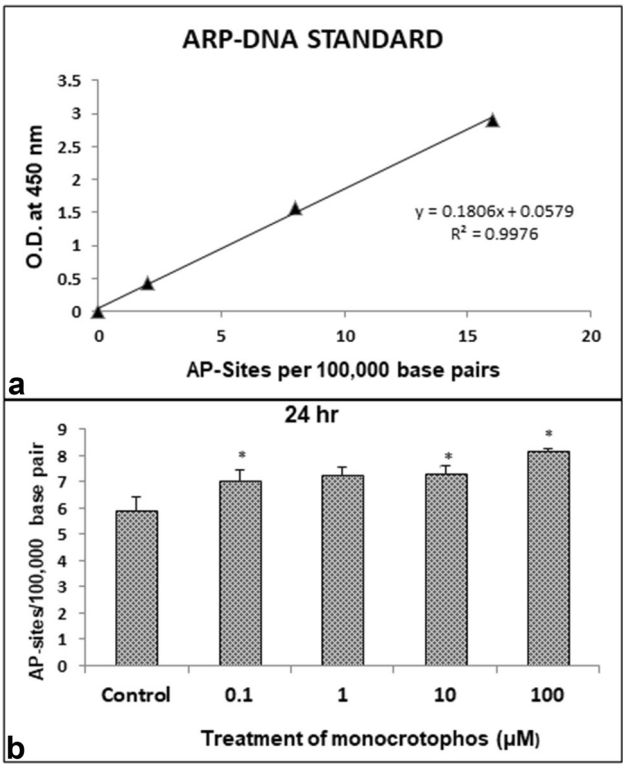

Fig. 3 Estimation of AP sites generated in A549 cells after treatment with monocrotophos (MCP). **a** ARP-DNA standard curve. **b** A549 cells were exposed to MCP (0.1, 1, 10 and 100 μM) for 24 h and the number of AP sites generated was measured using OxiSelect DNA damage (AP sites) detection kit. Results were expressed as number of AP sites/100,000 base pairs relative to untreated control cells ± standard deviation ($n = 3$; *P value <0.05)

Western blot analysis

BER-pathway is a frontline cellular approach to DNA repair against oxidative DNA damage and thus any alteration in the expression levels of BER enzymes can lead to the pathologic condition like cancer. Therefore, it is important to critically study all enzymes involved in the BER-pathway. In this study, APE1, OGG1, PARP1, XRCC1 and DNA pol β expression was explored in A549 cells treated with the OPPs CP and MCP. CP-induced changes in the protein expression levels of BER-pathway enzymes are presented in Fig. 5a. As compared to the vehicle control, APE1, PARP1, XRCC1 and DNA pol β were found to be upregulated after treatment with 10 and 100 μM CP for 24 h. Notably, for 48 h exposure, dose-dependent (1, 10 and 100 μM) upregulation was observed for DNA pol β, but the expression of APE1 and XRCC1 remained moderately changed. Interestingly, the DNA glycosylase OGG1 level was markedly reduced at both 24 and 48 h time points. For a long exposure (i.e. 72 h) to CP, an increase in the expression level was observed for PARP1, OGG1 and XRCC1, but the levels remained almost constant for APE1 and DNA pol β enzymes.

MCP-induced changes in the protein expression levels of BER-pathway enzymes are presented in Fig. 5b. The expression levels of APE1 were found to be significantly increased after 24, 48 and 72 h, with a maximum increase at moderate MCP concentrations of 1 and 10 μM (3- and 5-fold, respectively) for 48 h exposure, whereas OGG1 and DNA pol β expression levels were found to be moderately changed. PARP1 expression level was remarkably increased at all concentrations for 24 and 72 h time points. XRCC1 expression was found to be moderately increased for 48 and 72 h time points. The possible reason for the observed results can be explained as follows: an increase in tightly regulated cellular levels of BER-pathway enzymes APE1, PARP1, XRCC1 and DNA pol β at 24 h corresponds to the extent of DNA damage and genetic instability caused by the treatment of OPPs. Taken together, it can be stated that increased BER-pathway protein expression levels may reflect their increased activities, which might help the A549 cells maintain cell survival. On the other side, stabilization in the expression levels of the same BER enzymes at certain time points may indicate the formation of repair complexes on damaged DNA. Decreased OGG1 levels reflect reduced OGG1 activity and hence might be an increased susceptibility to lung cancer progression. Considering the observed results and the unique role of every BER enzyme in the BER-pathway capacity, it can be stated that the OPPs CP and MCP have the potential to induce enough defects/alterations in the BER-pathway that may play a role in lung carcinogenesis.

Determination of translational levels of transcription factors c-jun and Nrf2 by Western blotting

An imperative character of APE1 is due to its remarkably multifunctional role; apart from the DNA repair function, another important function of APE1 is redox regulation of various key cell survival TFs. The altered expression of TFs, c-jun, phospho-c-jun (p-c-jun) and Nrf2, and inducible nitric oxide synthase 2 (NOS2) have been associated with cancer development, progression and aggressiveness under the conditions of oxidative stress. Therefore, it was hypothesized to document the changes in c-jun, p-c-jun and Nrf2, and NOS2 expression levels after treatment with different concentrations of CP and MCP for various time points to understand the plausible link between APE1-regulated gene expression and lung cancer cell behaviour against CP- and MCP-induced oxidative stress.

CP-induced changes in the protein expression levels of TFs in A549 cells are presented in Fig. 6a. The TF c-jun expression was found to be significantly increased after treatment with 10 and 100 μM CP for 72 h. However, p-c-jun expression was found to be upregulated mainly at 24

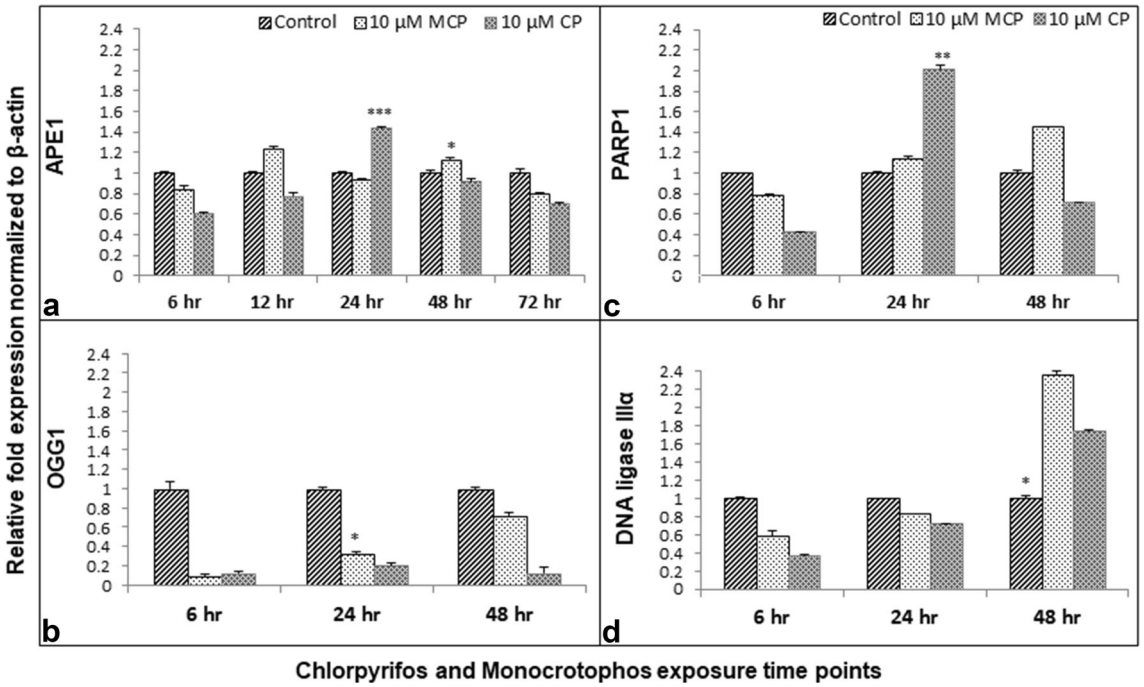

Fig. 4 Transcriptional changes in BER-pathway enzymes in chlorpyrifos (CP)- and monocrotophos (MCP)-treated A549 cells. Cells were exposed to CP and MCP (10 μM) for 6, 24 and 48 h, and qRT-PCR was performed to determine the *mRNA* expression levels of **a** *APE1*, **b** *PARP1*, **c** *OGG1* and **d** *DNA ligase III* α. Each mRNA expression is normalized to the internal control β-actin gene and presented as ± standard deviation ($n = 3$; $^{*}P$ value < 0.05, $^{**}P$ value < 0.01 and $^{***}P$ value <0.001)

and 48 h time points. As expected, the expression level of NOS2 was significantly increased by 1.8- and 1.7-fold for 10 and 100 μM of CP treatment for 24 h, whereas dose-dependent upregulation corresponding to 1.7-, 2-, 4- and 5-fold at 0.1, 1, 10 and 100 μM CP treatment, respectively, was observed at the 72 h time point. The Nrf2 protein expression remained unchanged at 0.1, 1 and 10 μM CP, but reduced to half (0.5-fold decrease) at a high concentration of 100 μM CP for 24 h of exposure. For 48 and 72 h of treatment, Nrf2 expression was increased by 1.2- and 1.4-fold (10 and 100 μM CP) and 1.5- and 1.4-fold (1 and 10 μM), respectively.

MCP-induced changes in the protein expression levels of TFs are presented in Fig. 6b. At 24 and 48 h time points, a remarkable upregulation in the expression level of c-jun was observed at 0.1 μM (2.6- and 3-fold), 1 μM (1.4- and 2.6-fold), 10 μM (2- and 2.6-fold) and 100 μM (1.6- and 3.4-fold), respectively. Exposure for 72 h also caused substantial upregulation at 1 and 10 μM (1.6 and 1.7, respectively). No change in the expression level of p-c-jun was observed at 24 h time point. However, moderate upregulation was seen at 100 μM MCP (1.3-fold) for 72 h exposure. Nrf2 expression was upregulated by 1.4-fold at 0.1 μM for 24 h, 2- and 1.8-fold at 1 and 10 μM for 48 h, and 1.2-, 1.4- and 1.2-fold at 1, 10 and 100 μM for 72 h time point. Altogether, these results suggest that in response to oxidative stress induced by the OPPs CP and MCP, the dysregulated c-jun, p-c-jun, NOS2 and Nrf2 expression along with disparity among BER-pathway enzymes may act as a potential determinant in lung cancer progression.

Immunofluorescence analysis of APE1 expression and subcellular localization against CP and MCP exposure

Next we investigated the subcellular localization of APE1 after exposure to OPPs, viz. CP and MCP, in A549 cells as a function of time. The cytoplasmic APE1 content was found to be gradually increased in CP-treated A549 cells when exposed to a low concentration of 0.01 μM for 6, 12 and 24 h (Fig. 7). Total APE1 was found to be significantly increased after treatment of A549 cells with both CP and MCP for 24 h. However, no change was observed after 48 h of treatment of A549 cells. These observations suggest that a low concentration of CP (0.01 μM) promotes cytoplasmic distribution of APE1 in A549 cells after 24 h of exposure, which might have been associated with the mitochondria or ER membranes or maintaining TFs in reduced state while they are being translocated to the nucleus. Consistent with the previous studies, APE1 was predominantly localized to the nuclei; however, the cytoplasmic APE1 was also detected significantly in the untreated control A549 cells at various time points studied.

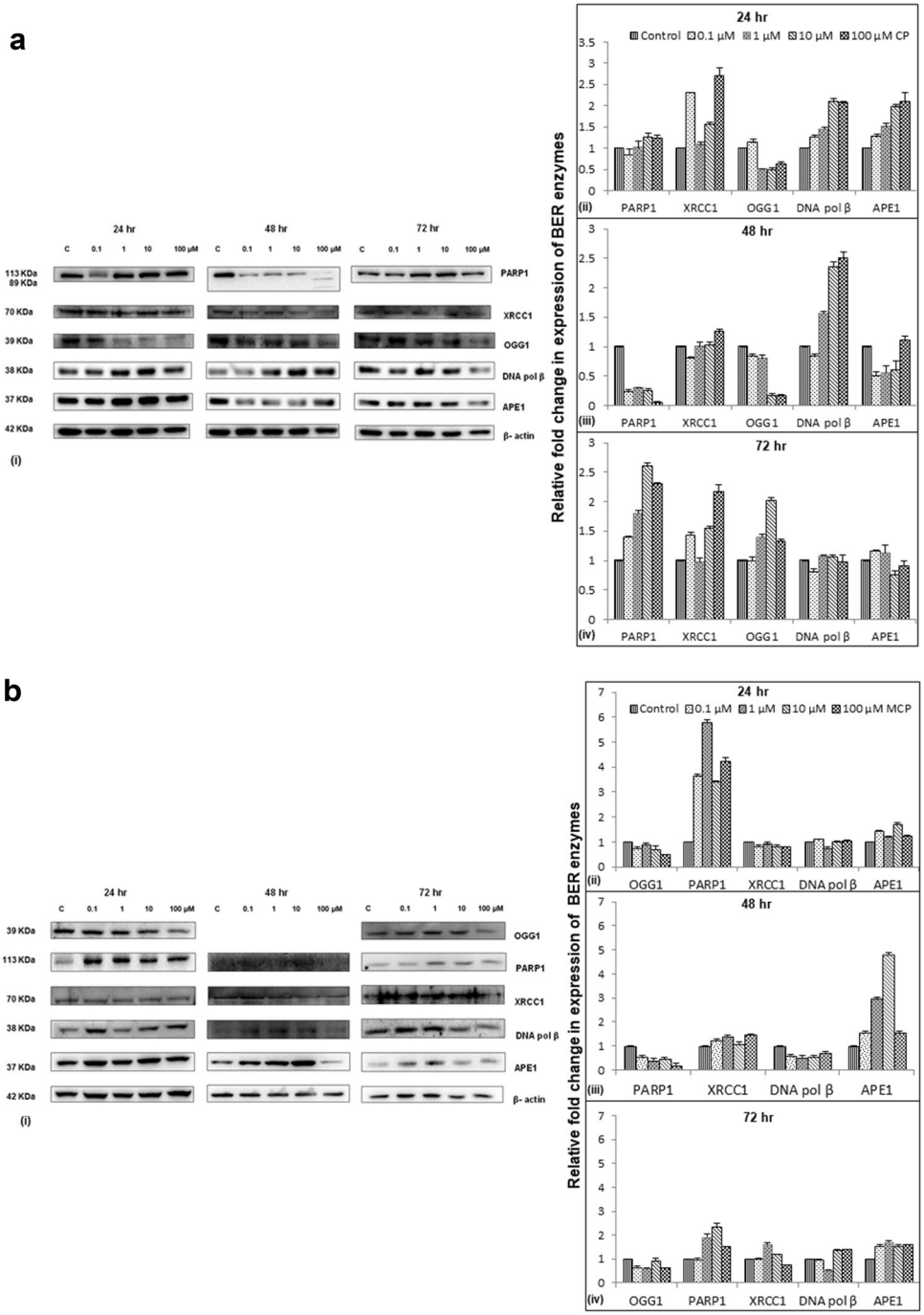

Fig. 5 Translational changes in BER-pathway enzymes in A549 cells after exposure to **a** chlorpyrifos (CP) and **b** monocrotophos (MCP). (i) A549 cells treated with 0.1, 1, 10 and 100 μM CP/MCP for 24, 48 and 72 h. Total cell lysates were prepared and Western blotting was performed to determine the protein expression levels of DNA repair BER-pathway enzymes, viz. PARP1, XRCC1, OGG1, DNA pol β and APE1. Each protein expression is normalized to the corresponding internal control β-actin and the best representative images are shown. (ii, iii and iv) Densitometric analysis of Western blotting of BER enzymes PARP1, XRCC1, OGG1, DNA pol β and APE1 normalized to β-actin, relative to the untreated control A549 cells exposed to CP/MCP for 24, 48 and 72 h. Data are expressed as fold change and mean ± standard error of mean (SEM) of two independent experiments ($n = 2$)

For MCP treatment, a significant reduction in the size of the nuclei and increased cytoplasmic APE1 were observed in A549 cells treated with a low concentration of 0.01 μM for 6 h. The APE1 immunoreactivity was significantly enhanced and distributed exclusively in the nuclei after 24 h of treatment with MCP. As the MCP treatment period was increased to 48 h, the APE1 immunoreactivity was significantly enhanced in both nuclear and cytoplasmic compartments of A549 cells. After treatment for 72 h with MCP, the total APE1 signal was found to be increased in A549 cells markedly with increased cytosolic APE1 content. The response observed in the case of 72 h of CP treatment was less as compared with that of MCP treatment in A549 cells. These observations suggest a possibility that a low concentration of MCP (0.01 μM) could stimulate (i) nuclear shrinking in A549 cells at 6 h, (ii) cytoplasm-to-nucleus translocation of APE1 in A549 cells at 24 h, (iii) peak levels of total APE1 signal (nuclear + cytoplasmic) at 48 h and (iv) a gradual increase of cytoplasmic APE1 at 6, 48 and 72 h. In addition, when the A549 cells were

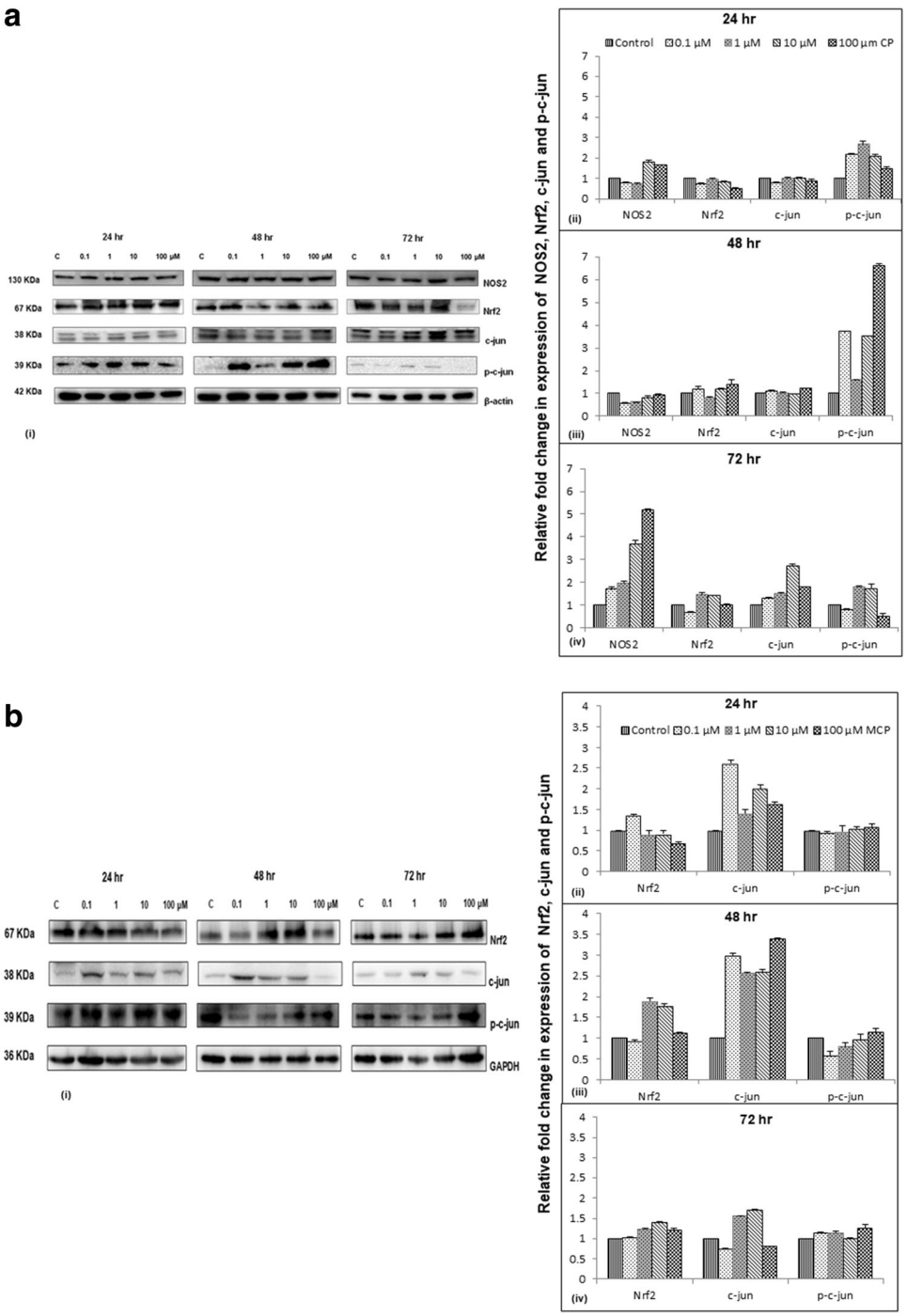

Fig. 6 Translational changes in TFs in A549 cells after exposure to **a** chlorpyrifos (CP) and **b** monocrotophos (MCP). (i) A549 cells were treated with 0.1, 1, 10 and 100 μM CP/MCP for 24, 48 and 72 h. Total cell lysates were prepared and Western blotting was performed to determine the expression levels of TFs, viz. NOS2, Nrf2, c-jun and p-c-jun. Each protein expression is normalized to the corresponding internal control β-actin and GAPDH, and the best representative images are shown. (ii, iii and iv) Densitometry analysis of Western blotting of NOS2, Nrf2, c-jun and p-c-jun, normalized to β-actin and GAPDH, relative to the untreated control A549 cells exposed to CP/MCP for 24 h, 48 h and 72 h. Data are expressed as fold change and mean ± standard error of mean (SEM) of two independent experiments ($n = 2$)

exposed to 10 μM concentrations of CP and MCP (Fig. 8), translocation of APE1 was observed within the cytoplasm of A549 cells at an early 6 h time point. However, the APE1 localization was found to be exclusively promoted to the nuclei after 24 h, and in the case of 48 h treatment, a reduced APE1 signal was observed. Therefore, it can be stated that OPP-induced subcellular distribution of APE1 is somewhat heterogenous within the cell subpopulation and is tightly regulated in response to oxidative stress.

Confocal laser scanning microscopic analysis for interaction between APE1 and c-jun

In the Results section, we have shown that APE1 is present in both the nucleus and the cytoplasm of A549 cells, but it was observed to be predominantly localized to the nuclei when exposed to CP and MCP for 24 and 48 h. Here we further examined the localization of APE1 along with TF c-jun in CP- and MCP-treated A549 cells after 6, 24 and

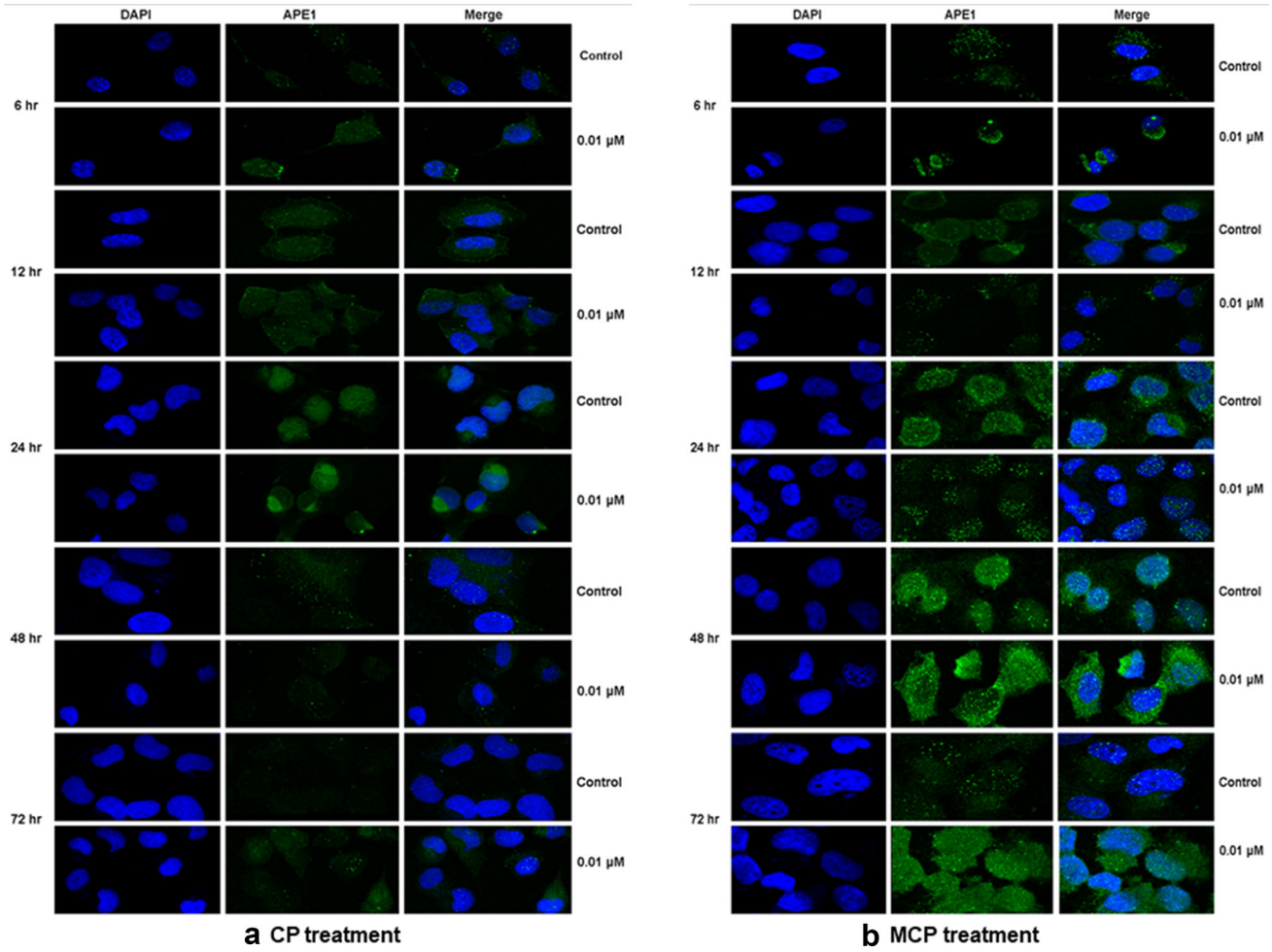

Fig. 7 **a** Chlorpyrifos (CP)- and **b** monocrotophos (MCP)-induced subcellular distribution of APE1 in A549 cells. The A549 cells were treated with a low concentration of 0.01 μM CP and MCP for 6, 12, 24, 48 and 72 h and the localization of APE1 was determined using immunofluorescence staining using APE1-specific antibody. Images were acquired at 60× using a FV1200 confocal laser scanning microscope (CLSM) (Olympus). A *scale bar* of 10 μm was used

48 h time points to illustrate the role of APE1 in redox-mediated c-jun regulation. As depicted in Fig. 9, APE1 and c-jun were found to be distributed in both the nucleus and the cytoplasm of A549 cells. The PCC values were used to quantify the degree of colocalization. As compared to untreated control A549 cells, no visible change in the expression and localization pattern of APE1 and c-jun was observed when exposed to 10 μM CP and MCP for 6 h. However, exposure for 24 h resulted in significant nuclear colocalization of APE1 with the TF c-jun, as evidenced by the PCC values 0.6 and 0.53 at 10 μM CP and MCP, respectively. In addition, as the exposure time was increased to 48 h, the treatment of 10 μM CP and MCP resulted in moderate nuclear and cytoplasmic colocalization of APE1 with c-jun, and the observed PCC values were 0.3 and 0.45, respectively. Taken together, these results indicate that APE1 interacts with the TF c-jun in the nucleus and regulates via its redox function to facilitate the activation of downstream gene expression.

Discussion

Till now, there has been limited information regarding the increased risk of lung cancer in people exposed to OPPs such as CP and MCP. Although some epidemiological studies suggest for the possible link between OPPs exposure and lung cancer [5, 6], not enough biochemical studies have been performed to confirm the same, thus leaving the data equivocal. There are gaps in our knowledge due to lack of detailed biochemical studies regarding the role of MCP and CP in lung cancer risk and the underlying molecular mechanisms. Considering the indispensable role of DNA repair and cell survival pathways in maintaining

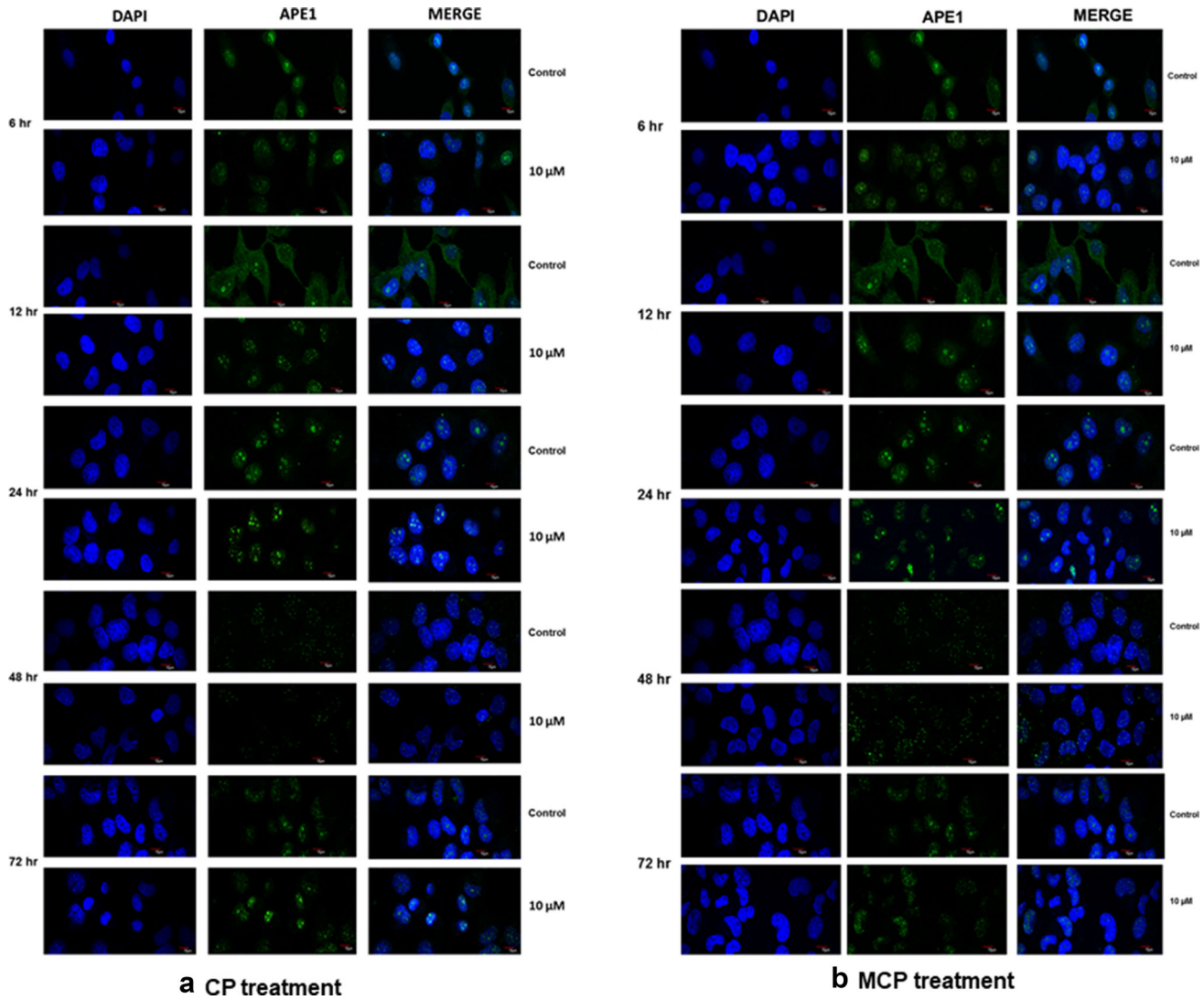

Fig. 8 **a** Chlorpyrifos (CP)- and **b** monocrotophos (MCP)-induced subcellular distribution of APE1 in A549 cells. The A549 cells were treated with an optimum (moderate) concentration of 10 μM CP and MCP for 6, 12, 24, 48 and 72 h and the localization of APE1 was determined using immunofluorescence staining using APE1-specific antibody. Images were acquired at 60× using a FV1200 confocal laser scanning microscope (CLSM) (Olympus). A *scale bar* of 10 μm was used

the cellular genomic integrity, we wished to explore the CP- and MCP-mediated alteration in DNA BER-pathway and other stress-responsive cell signalling pathways, which may be involved in the pathogenesis of lung cancer. The results of the present study suggest that low and moderate dose exposure to OPPs MCP and CP increases lung cancer risk by virtue of ROS-mediated suboptimal DNA repair due to imbalanced BER-pathway and increased cell survival because of activation of pro-survival signalling pathways and also by the means of BER-pathway's key enzyme APE1-mediated redox regulation of TFs crucial for the growth of lung carcinoma cells.

Cytotoxic effects of MCP have been evaluated in different mammalian cell lines and have been demonstrated to cause cancer cell proliferation [8, 34, 35]. A study reported that CP is cytotoxic at >250 μM in A549 cells [26]. From our results, as evidenced by MTT assay, CP and MCP showed cytotoxicity only at higher concentration (500 μM), whereas non-toxic lower concentrations (10 and 100 μM) resulted in increased cell viability at 24 and 48 h. Our results indicate that lower non-cytotoxic doses of CP and MCP generate intracellular ROS in A549 cells as early as 6 h, but a maximum increase was observed at 10 μM after 24 h of treatment. Studies have demonstrated that OPPs have the potential to cause oxidative stress by generating ROS [28, 36]. In our study, this increased ROS generation at non-cytotoxic concentrations of CP and MCP in A549 cells might be considered as a likely mechanism underlying the activation of pro-survival signalling

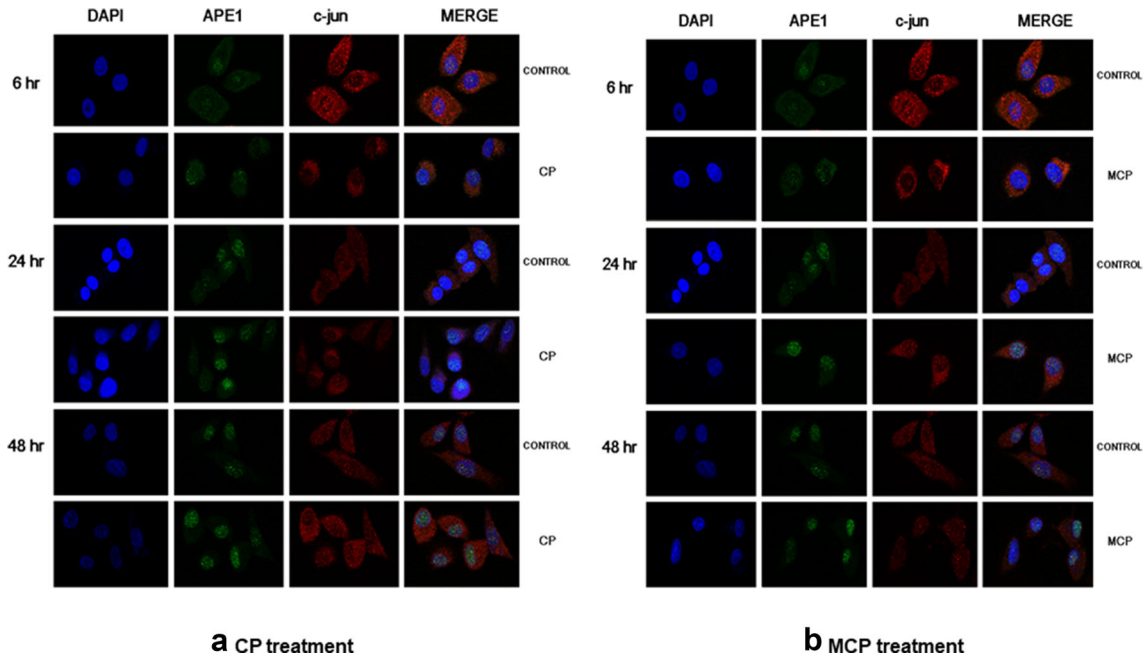

Fig. 9 **a** Chlorpyrifos (CP)- and **b** monocrotophos (MCP)-induced subcellular distribution and colocalization of APE1 and the TF c-jun in A549 cells. The A549 cells were treated with 10 μM CP and MCP for 24, 48 and 72 h, and the subcellular distribution and also colocalization of APE1 and the TF c-jun were determined using immunofluorescence staining using specific antibodies against these two proteins. The images were acquired at 60× using a FV1200 confocal laser scanning microscope (CLSM) (Olympus). A *scale bar* of 10 μm was used

pathways and this may be an important factor involved in increased cancer cell proliferation.

Oxidative stress manifests into oxidative DNA base damage. AP sites are the most frequently found form of mutagenic DNA base damage lesions generated by ROS [37]. Our study observed the accumulation of AP sites in response to MCP treatment in A549 cells, pointing towards the extent of DNA damage. These mutagenic AP sites are processed by APE1-dependent DNA repair BER-pathway. In response to oxidative DNA damage, BER-pathway, an evolutionarily conserved and environmentally responsive mechanism, gets activated in which five major enzymes execute the process. First, DG OGG1-mediated identification/excision of damaged base takes place, which generates the AP site; it involves the processing of generated AP site by APE1 and finally the completion of DNA repair process by "short-patch" or "long-patch" pathway utilizing XRCC1, DNA pol β, DNA ligase III α or DNA ligase I [14, 38]. Our study is focused on "short-patch" BER-pathway. Various studies have demonstrated that individual BER-pathway enzymes get induced in response to oxidative stress [39, 40]. In our study, qRT-PCR and Western blotting analyses demonstrated a decrease in mRNA and protein expression of OGG1 at all time points in A549 cells exposed to CP and MCP. The downregulated OGG1 protein expression may indicate the suppression of DNA damage repair, causing DNA damage to accumulate. A previous study has reported the link between low OGG1 expression and increased lung cancer risk [16]. On the contrary, the levels of APE1, PARP1, XRCC1 and DNA pol β were found to be significantly increased after exposure to CP for 24 h. It is well known that PARP1 acts as a DNA damage sensor and positively regulates DNA repair process by recruiting the downstream DNA repair enzymes at the site of DNA damage, whereas XRCC1 acts as a scaffold to allow protein–protein interactions and DNA pol β helps in gap-filling synthesis at AP sites [41, 42]. Taking into account the important role of every BER-pathway enzyme in DNA repair, the observed results positively advocate that the CP exposure induced enough oxidative DNA damage in the A549 cells to stimulate changes in the expression of tightly regulated DNA BER-pathway proteins. The observed results in MCP-treated A549 cells were found to be similar, except for XRCC1 and DNA pol β expression, which remained moderately increased or unchanged. Here, stabilization in the expression levels of the same BER enzymes may indicate the formation of repair complexes on damaged DNA or it may point towards the possibility of less efficient DNA repair or misincorporations of nucleotides, which may result in increased mutagenesis rate [43, 44]. Coordination between the BER-pathway enzymes is crucial; for example, DNA pol β lacks proofreading activity and cannot correct the misincorporations; hence, such misincorporations are

corrected by the 3′–5′ exonuclease activity of APE1 [45, 46]. Considering the fact that APE1 functions by creating single-strand breaks (SSBs) in DNA during the repair process, it should come as no surprise that this break can become mutagenic if not processed correctly by impaired APE1 or other downstream BER enzymes. Therefore, dysregulation and imbalance in APE1 and other BER enzymes has been linked with cancer [47]. Although it is important to determine overall BER activity against oxidative stress, it is definitely not necessary to observe the dysregulation of complete BER-pathway enzymes to establish its role in causing genomic instability. Alteration in any one enzymatic step of BER-pathway can lead to cellular transformation. The opposing alterations or imbalance in BER-pathway proteins that we typically observed in both CP- and MCP-treated A549 cells potentially reflects the dysregulated BER-pathway proteins and their altered enzymatic activities, which might be contributing to carcinogenesis.

Among all BER-pathway proteins, our study holds special interest in APE1 because of its second important function as a redox regulator of various TFs involved in cellular stress responses and cell survival mechanisms. The TF c-jun (AP-1) has been known to be induced by oxidative stress and redox-regulated by APE1 [17, 19, 48]. It has been reported to be involved in BER-pathway gene regulation [49] and frequently expressed in lung cancer [50]. As evidenced by immunoblotting, our study showed a significant increase in the expression level of c-jun, which has been considered to be associated with proliferation and angiogenesis in cancer [51, 52]. A study has shown that the activation of AP-1 signalling pathway involving both c-jun and p-c-jun promotes cell proliferation in lung cancer [53]. The phosphorylation of c-jun activates c-jun-dependent transcription. A study has shown that binding of p-c-jun to vascular endothelial growth factor (VEGF) promoter activates VEGF transcription which triggers angiogenesis in cancer [54]. Another study reported that HPV-16 E7 oncoprotein enhances p-c-jun expression in A549 cells, which along with c-jun is involved in inducing HIF-1α, VEGF and IL-8 expression and thus stimulating angiogenesis [55]. Consistent with these findings, our results also demonstrate the increased expression of p-c-jun (Ser 63), indicating that c-jun- and p-c-jun-mediated pathway is somehow involved in cell survival mechanisms in response to CP- and MCP-induced oxidative stress.

Also the NOS2 expression was found to be increased in A549 cells exposed to CP. NOS2 stimulates the production of NO which is an inflammatory mediator. Sustained NO production has been linked with carcinogenesis which, with inhibition of BER-pathway enzyme OGG1, could contribute to the development of mutagenic environment for chronic inflammation [56]. Another important TF that we intended to combine with our study was Nrf2. As an important stress-responsive TF, Nrf2 plays a very important role in protecting cells from apoptosis and oxidative stress via activation of anti-oxidant proteins [57]. In recent years, there has been considerable debate over the dual role of Nrf2 in cancer, suggesting that hyperactivation of Nrf2 confers survival advantage to cancer cells [58, 59]. Nrf2 plays a pro-tumorigenic role in early stages of promotion and progression of lung cancer [60]. Studies have reported the association between dysregulated Nrf2 signal and lung cancer [61, 62]. In our study, CP- and MCP-induced oxidative stress was found to significantly increase the Nrf2 protein expression at certain time points, which meant that the activation of Nrf2-mediated signalling pathway(s) protects the cells from further oxidative stress and also helps in cell proliferation.

Moreover, the altered subcellular localization of APE1 has been associated with lung cancer progression [25, 63]. Therefore, we examined the changes in subcellular localization of APE1 in A549 cells exposed to the OPPs CP and MCP, using CLSM analysis. Our study showed the cytoplasmic translocation of an early time point of 6 h; however, it was found to be exclusively promoted in the nuclei after 24 h. These observations point towards the heterogenous and differential subcellular distribution of APE1 against oxidative stress. Again, immunofluorescence analysis using CLSM was performed to determine whether CP- and MCP-induced oxidative stress stimulates the TF c-jun via APE1 signalling pathway. Because colocalization of APE1 with TFs c-jun is also thought to contribute towards the APE1-mediated transcriptional regulation of c-jun, we next demonstrated the subcellular colocalization pattern of APE1 and c-jun in A549 cells exposed to CP and MCP. Analysis of colocalization was performed by calculating PCC values; our results showed a positive correlation in nuclear localization of APE1 and c-jun in cellular response to CP- and MCP-induced oxidative stress. A previous study has also shown that the nuclear expression of p-c-jun has an important role in human colorectal tumour development [64]. Taken together, these results may support the hypothesis that in response to CP- and MCP-induced oxidative stress the nuclear functional interaction of APE1 with c-jun is involved in the activation of c-jun signalling pathway which ultimately promotes lung carcinogenesis.

In conclusion, our study suggests that the OPPs CP and MCP have the potential to cause oxidative stress and oxidative DNA damage in A549 cells. This OPP-mediated oxidative stress alters the BER-pathway and the stress response of TFs c-jun, p-c-jun and Nrf2, and modulates APE1's subcellular localization and redox regulation of TFs. Our results indicate that in response to CP- and MCP-induced ROS in A549 cells, APE1 acts as a potential player

in both the instances; first as a repair enzyme of BER-pathway and second as a redox regulator of pivotal TFs involved in pro-survival mechanisms; thus, it ensures the survival and proliferation of lung cancer cells and ultimately contributes to the process of lung carcinogenesis. Besides its role in carcinogenesis, APE1-mediated functions may even revamp tumour response to therapy. For that reason, further investigations are required to reveal APE1's prospect for development of chemotherapeutics against lung cancer.

Acknowledgements This work was supported by the BSR-startup Grant from the University Grants Commission (UGC), New Delhi, India, and the funds received under the scheme Research Seed Money (RSM) from the Central University of Punjab, Bathinda (CUPB) to A.K.M. A.K.M. also acknowledges the training in the field of BER-pathway and Redox biology under the guidance of Prof. Sankar Mitra at University of Texas Medical Branch, Galveston, Texas, USA. S.T. acknowledges the financial support in the form of Senior Research Fellowship (SRF) from the Indian Council of Medical Research (ICMR), New Delhi, India. Central Instrumentation Laboratory (CIL) facility of CUPB is thankfully acknowledged for providing confocal microscopy facility. Because of the limited focus of the article, many relevant and appropriate references could not be included, for which the authors apologize.

Compliance with ethical standards

Conflict of interest The authors declare that no conflict of interest exists.

References

1. Kisby GE, Muniz JF, Scherer J, Lasarev MR, Koshy M, Kow YW, McCauley L (2009) Oxidative stress and DNA damage in agricultural workers. J Agromedicine 14:206–214
2. Ojha A, Srivastava N (2014) In vitro studies on organophosphate pesticides induced oxidative DNA damage in rat lymphocytes. Mutat Res, Genet Toxicol Environ Mutagen 761:10–17
3. Kamel F, Hoppin JA (2004) Association of pesticide exposure with neurologic dysfunction and disease. Environ Health Perspect 112:950–958
4. Raanan R, Harley KG, Balmes JR, Bradman A, Lipsett M, Eskenazi B (2015) Early-life exposure to organophosphate pesticides and pediatric respiratory symptoms in the CHAMACOS cohort. Environ Health Perspect 123:179
5. Lee WJ, Blair A, Hoppin JA, Lubin JH, Rusiecki JA, Sandler DP, Dosemeci M, Alavanja MC (2004) Cancer incidence among pesticide applicators exposed to chlorpyrifos in the agricultural health study. J Natl Cancer Inst 96:1781–1789
6. Alavanja MC, Dosemeci M, Samanic C, Lubin J, Lynch CF, Knott C, Barker J, Hoppin JA, Sandler DP, Coble J (2004) Pesticides and lung cancer risk in the agricultural health study cohort. Am J Epidemiol 160:876–885
7. Y-l Zhou, J-g Yan, C-l Sun (2009) DNA damage of monocrotophos on mice. J Xinxiang Med Col 26:141–144
8. Isoda H, Talorete T, Han J, Oka S, Abe Y, Inamori Y (2004) Effects of organophosphorous pesticides used in china on various mammalian cells. Environ Sci 12:9–19
9. Kashyap M, Singh A, Siddiqui M, Kumar V, Tripathi V, Khanna V, Yadav S, Jain S, Pant A (2010) Caspase cascade regulated mitochondria mediated apoptosis in monocrotophos exposed PC12 cells. Chem Res Toxicol 23:1663–1672
10. Cui Y, Guo J, Xu B, Chen Z (2011) Genotoxicity of chlorpyrifos and cypermethrin to ICR mouse hepatocytes. Toxicol Mech Method 21:70–74
11. Rahman M, Mahboob M, Danadevi K, Banu BS, Grover P (2002) Assessment of genotoxic effects of chloropyriphos and acephate by the comet assay in mice leucocytes. Mutat Res 516:139–147
12. Chauhan LK, Varshney M, Pandey V, Sharma P, Verma VK, Kumar P, Goel SK (2016) ROS-dependent genotoxicity, cell cycle perturbations and apoptosis in mouse bone marrow cells exposed to formulated mixture of cypermethrin and chlorpyrifos. Mutagenesis 31:635–642
13. Prasad R, Horton JK, Liu Y, Wilson SH (2016) Central steps in mammalian BER and regulation by PARP1. In: Wilson DM III (ed) The base excision repair pathway: molecular mechanisms and role in disease development and therapeutic design. World Scientific, New Jersey, pp 253–280
14. Hegde ML, Hazra TK, Mitra S (2008) Early steps in the DNA base excision/single-strand interruption repair pathway in mammalian cells. Cell Res 18:27–47
15. Thakur S, Sarkar B, Cholia RP, Gautam N, Dhiman M, Mantha AK (2014) APE1/ref-1 as an emerging therapeutic target for various human diseases: phytochemical modulation of its functions. Exp Mol Med 46:e106
16. Paz-Elizur T, Krupsky M, Blumenstein S, Elinger D, Schechtman E, Livneh Z (2003) DNA repair activity for oxidative damage and risk of lung cancer. J Natl Cancer Inst 95:1312–1319
17. Bhakat KK, Mantha AK, Mitra S (2009) Transcriptional regulatory functions of mammalian AP-endonuclease (APE1/Ref-1), an essential multifunctional protein. Antioxid Redox Signal 11:621–637
18. Fishel ML, Wu X, Devlin CM, Logsdon DP, Jiang Y, Luo M, He Y, Yu Z, Tong Y, Lipking KP (2015) Apurinic/apyrimidinic endonuclease/redox factor-1 (APE1/Ref-1) redox function negatively regulates NRF2. J Biol Chem 290:3057–3068
19. Tell G, Quadrifoglio F, Tiribelli C, Kelley MR (2009) The many functions of APE1/Ref-1: not only a DNA repair enzyme. Antioxid Redox Signal 11:601–619
20. Woo J, Park H, Sung SH, Moon B-I, Suh H, Lim W (2014) Prognostic value of human apurinic/apyrimidinic endonuclease 1 (APE1) expression in breast cancer. PLoS ONE 9:e99528
21. Kelley MR, Cheng L, Foster R, Tritt R, Jiang J, Broshears J, Koch M (2001) Elevated and altered expression of the multifunctional DNA base excision repair and redox enzyme Ape1/ref-1 in prostate cancer. Clin Cancer Res 7:824–830
22. Sevilya Z, Leitner-Dagan Y, Pinchev M, Kremer R, Elinger D, Lejbkowicz F, Rennert HS, Freedman LS, Rennert G, Paz-Elizur T (2015) Development of APE1 enzymatic DNA repair assays: low APE1 activity is associated with increase lung cancer risk. Carcinogenesis 36:982–991
23. Yoo DG, Song YJ, Cho EJ, Lee SK, Park JB, Yu JH, Lim SP, Kim JM, Jeon BH (2008) Alteration of APE1/ref-1 expression in non-small cell lung cancer: the implications of impaired extracellular superoxide dismutase and catalase antioxidant systems. Lung Cancer 60:277–284
24. Tell G, Damante G, Caldwell D, Kelley MR (2005) The intracellular localization of APE1/Ref-1: more than a passive phenomenon? Antioxid Redox Signal 7:367–384
25. Puglisi F, Aprili G, Minisini A (2001) Prognostic significance of Ape1/ref-1 subcellular localization in non-small cell lung carcinomas. Anticancer Res 21:4041–4050
26. Oostingh GJ, Wichmann G, Schmittner M, Lehmann I, Duschl A (2009) The cytotoxic effects of the organophosphates chlorpyrifos and diazinon differ from their immunomodulating effects. J Immunotoxicol 6:136–145

27. Gong J, Muñoz AR, Chan D, Ghosh R, Kumar AP (2014) STAT3 down regulates LC3 to inhibit autophagy and pancreatic cancer cell growth. Oncotarget 5:2529–2541
28. Kashyap MP, Singh AK, Kumar V, Tripathi VK, Srivastava RK, Agrawal M, Khanna VK, Yadav S, Jain SK, Pant AB (2011) Monocrotophos induced apoptosis in PC12 cells: role of xenobiotic metabolizing cytochrome P450s. PLoS ONE 6:e17757
29. Gill I, Kaur S, Kaur N, Dhiman M, Mantha AK (2017) Phytochemical ginkgolide B attenuates amyloid-β1-42 induced oxidative damage and altered cellular responses in human neuroblastoma SH-SY5Y cells. J Alzheimer's Dis. doi:10.3233/JAD-161086
30. Vaday GG, Peehl DM, Kadam PA, Lawrence DM (2006) Expression of CCL5 (RANTES) and CCR5 in prostate cancer. Prostate 66:124–134
31. Mantha AK, Dhiman M, Taglialatela G, Perez-Polo RJ, Mitra S (2012) Proteomic study of amyloid beta (25–35) peptide exposure to neuronal cells: impact on APE1/Ref-1′s protein–protein interaction. J Neurosci Res 90:1230–1239
32. Zhao J, Zhang J, Yu M, Xie Y, Huang Y, Wolff DW, Abel PW, Tu Y (2013) Mitochondrial dynamics regulates migration and invasion of breast cancer cells. Oncogene 32:4814–4824
33. Dunn KW, Kamocka MM, McDonald JH (2011) A practical guide to evaluating colocalization in biological microscopy. Am J Physiol Cell Physiol 300:C723–C742
34. Isoda H, Talorete TP, Han J, Oka S, Abe Y, Inamori Y (2005) Effects of organophosphorous pesticides used in china on various mammalian cells. Environ Sci 12:9–19
35. Lu XT, Ma Y, Wang C, Zhang XF, Jin DQ, Huang CJ (2012) Cytotoxicity and DNA damage of five organophosphorus pesticides mediated by oxidative stress in PC12 cells and protection by vitamin E. J Environ Sci Health B 47:445–454
36. Edwards FL, Yedjou CG, Tchounwou PB (2013) Involvement of oxidative stress in methyl parathion and parathion-induced toxicity and genotoxicity to human liver carcinoma (HepG2) cells. Environ Toxicol 28:342–348
37. Nakamura J, La DK, Swenberg JA (2000) 5′-Nicked apurinic/apyrimidinic sites are resistant to β-elimination by β-polymerase and are persistent in human cultured cells after oxidative stress. J Biol Chem 275:5323–5328
38. Wilson D 3rd, Sofinowski T, McNeill D (2003) Repair mechanisms for oxidative DNA damage. Front Biosci 8:d963–981
39. Cabelof DC, Raffoul JJ, Yanamadala S, Guo Z, Heydari AR (2002) Induction of DNA polymerase β-dependent base excision repair in response to oxidative stress in vivo. Carcinogenesis 23:1419–1425
40. Izumi T, Wiederhold LR, Roy G, Roy R, Jaiswal A, Bhakat KK, Mitra S, Hazra TK (2003) Mammalian DNA base excision repair proteins: their interactions and role in repair of oxidative DNA damage. Toxicology 193:43–65
41. Horton JK, Watson M, Stefanick DF, Shaughnessy DT, Taylor JA, Wilson SH (2008) XRCC1 and DNA polymerase β in cellular protection against cytotoxic DNA single-strand breaks. Cell Res 18:48–63
42. Ko HL, Ren EC (2012) Functional aspects of PARP1 in DNA repair and transcription. Biomolecules 2:524–548
43. Dianov GL, Hübscher U (2013) Mammalian base excision repair: the forgotten archangel. Nucl Acids Res 41:3483–3490
44. Hegde ML, Izumi T, Mitra S (2012) Oxidized base damage and single-strand break repair in mammalian genomes: role of disordered regions and posttranslational modifications in early enzymes. Prog Mol Biol Transl Sci 110:123
45. Sukhanova MV, Khodyreva SN, Lebedeva NA, Prasad R, Wilson SH, Lavrik OI (2005) Human base excision repair enzymes apurinic/apyrimidinic endonuclease1 (APE1), DNA polymerase β and poly (ADP-ribose) polymerase 1: interplay between strand-displacement DNA synthesis and proofreading exonuclease activity. Nucl Acids Res 33:1222–1229
46. Wong D, Demple B (2004) Modulation of the 5′-deoxyribose-5-phosphate lyase and DNA synthesis activities of mammalian DNA polymerase β by apurinic/apyrimidinic endonuclease 1. J Biol Chem 279:25268–25275
47. Poletto M, Legrand AJ, Fletcher SC, Dianov GL (2016) p53 coordinates base excision repair to prevent genomic instability. Nucl Acids Res 44:3165–3175
48. Xanthoudakis S, Miao G, Wang F, Pan Y-C, Curran T (1992) Redox activation of Fos-Jun DNA binding activity is mediated by a DNA repair enzyme. EMBO J 11:3323
49. Christmann M, Kaina B (2013) Transcriptional regulation of human DNA repair genes following genotoxic stress: trigger mechanisms, inducible responses and genotoxic adaptation. Nucl Acids Res 41:8403–8420
50. Maeno K, Masuda A, Yanagisawa K, Konishi H, Osada H, Saito T, Ueda R, Takahashi T (2006) Altered regulation of c-jun and its involvement in anchorage-independent growth of human lung cancers. Oncogene 25:271–277
51. Zhang G, Dass CR, Sumithran E, Di Girolamo N, Sun L-Q, Khachigian LM (2004) Effect of deoxyribozymes targeting c-Jun on solid tumor growth and angiogenesis in rodents. J Natl Cancer Inst 96:683–696
52. Vleugel MM, Greijer AE, Bos R, van der Wall E, van Diest PJ (2006) c-Jun activation is associated with proliferation and angiogenesis in invasive breast cancer. Hum Pathol 37:668–674
53. Zhang S, Hu Y, Huang Y, Xu H, Wu G, Dai H (2015) Heat shock protein 27 promotes cell proliferation through activator protein-1 in lung cancer. Oncology Lett 9:2572–2576
54. Yin Y, Wang S, Sun Y, Matt Y, Colburn NH, Shu Y, Han X (2009) JNK/AP-1 pathway is involved in tumor necrosis factor-α induced expression of vascular endothelial growth factor in MCF7 cells. Biomed Pharmacother 63:429–435
55. Zhang E, Feng X, Liu F, Zhang P, Liang J, Tang X (2014) Roles of PI3 K/Akt and c-Jun signaling pathways in human papillomavirus type 16 oncoprotein-induced HIF-1α, VEGF, and IL-8 expression and in vitro angiogenesis in non-small cell lung cancer cells. PLoS ONE 9:e103440
56. Jaiswal M, LaRusso NF, Nishioka N, Nakabeppu Y, Gores GJ (2001) Human Ogg1, a protein involved in the repair of 8-oxoguanine, is inhibited by nitric oxide. Cancer Res 61:6388–6393
57. Kim SK, Yang JW, Kim MR, Roh SH, Kim HG, Lee KY, Jeong HG, Kang KW (2008) Increased expression of Nrf2/ARE-dependent anti-oxidant proteins in tamoxifen-resistant breast cancer cells. Free Radic Biol Med 45:537–546
58. Lau A, Villeneuve NF, Sun Z, Wong PK, Zhang DD (2008) Dual roles of Nrf2 in cancer. Pharmacol Res 58:262–270
59. Sporn MB, Liby KT (2012) NRF2 and cancer: the good, the bad and the importance of context. Nat Rev Cancer 12:564–571
60. Alexander C-M (2013) The involvement of NRF2 in lung cancer. Oxid Med Cell Longev 2013:746432
61. Tian Y, Liu Q, He X, Yuan X, Chen Y, Chu Q, Wu K (2016) Emerging roles of Nrf2 signal in non-small cell lung cancer. J Hematol Oncol 9:14
62. Homma S, Ishii Y, Morishima Y, Yamadori T, Matsuno Y, Haraguchi N, Kikuchi N, Satoh H, Sakamoto T, Hizawa N (2009) Nrf2 enhances cell proliferation and resistance to anticancer drugs in human lung cancer. Clin Cancer Res 15:3423–3432
63. Wu H, Cheng Y, Chang J, Wu T, Liu W, Chen C, Lee H (2010) Subcellular localization of apurinic endonuclease 1 promotes lung tumor aggressiveness via NF-κB activation. Oncogene 29:4330–4340
64. Takeda K, Kinoshita I, Shimizu Y, Ohba Y, Itoh T, Matsuno Y, Shichinohe T, Dosaka-Akita H (2008) Clinicopathological significance of expression of pc-Jun, TCF4 and beta-Catenin in colorectal tumors. BMC Cancer 8:328